

**NANO EXPRESS**

**Open Access**

# Conjugate heat transfer of laminar mixed convection of a nanofluid through an inclined tube with circumferentially non-uniform heating

Shahriar Allahyari<sup>1</sup>, Amin Behzadmehr<sup>1\*</sup> and Seyed Masoud Hosseini Sarvari<sup>2</sup>

## Abstract

Laminar mixed convection of a nanofluid consisting of water and  $\text{Al}_2\text{O}_3$  in an inclined tube with heating at the top half surface of a copper tube has been studied numerically. The bottom half of the tube wall is assumed to be adiabatic (presenting a tube of a solar collector). Heat conduction mechanism through the tube wall is considered. Three-dimensional governing equations with using two-phase mixture model have been solved to investigate hydrodynamic and thermal behaviours of the nanofluid over wide range of nanoparticle volume fractions. For a given nanoparticle mean diameter the effects of nanoparticle volume fractions on the hydrodynamics and thermal parameters are presented and discussed at different Richardson numbers and different tube inclinations. Significant augmentation on the heat transfer coefficient as well as on the wall shear stress is seen.

## Introduction

Many different industries such as electronic, automotive and aerospace have been facing heat transfer limitation for improving performance of their thermal systems. Heat transfer enhancement has been considered as one of the key parameter for developing more efficient and effective thermal devices. Thus this issue has been studied extensively. Different active and passive methods have been considered for the heat transfer augmentation. Improving the thermo-physical properties of the working fluids such as water, oil and ethylene glycol mixture is one of the possible methods. Therefore, there has been a strong motivation to develop a new heat transfer fluids with substantially higher thermal conductivity. Choi [1] presented a new generation of solid-liquid mixtures that is called nanofluid. It demonstrates significant improvement over the thermal characteristics of the base fluids. Various nanofluids with different nanoparticle and base fluid materials have been prepared and their thermo-fluid characteristics have been investigated by many researchers.

Among them, experimental studies of [2-5] on confined geometries could be cited. In general they found

that the Nusselt number increases with the nanoparticle concentrations and significant heat transfer enhancement has been achieved. Many works have been dedicated to determine and model the effective physical properties of different nanofluid. For instance, investigations of Refs. [6-13] on the effective thermal conductivity or the works that have been done by [14,15] on the nanofluid effective viscosity could be mentioned.

Convective heat transfer with nanofluids can be modelled using the two-phase or single-phase approach. The first provides the possibility of understanding the function of both the fluid phase and the solid particles in the heat transfer mechanisms. The second assumes that the fluid phase and particle are in thermal and hydrodynamic equilibrium. This approach is simpler and requires less computational time. Thus it has been used in several theoretical studies of convective heat transfer with nanofluids [16-18]. However, the concerns in single-phase modelling consist in selecting the proper effective properties for nanofluids and taking into account the chaotic movement of ultra fine particle. To partially overcome this difficulty, some researches [19-21] used the dispersion model which takes into account the improvement of heat transfer due to the random movement of particles in the main flow. In addition several factors such as gravity, friction between the fluid and solid particles and Brownian forces, the phenomena of

\* Correspondence: amin.behzadmehr@eng.usb.ac.ir

<sup>1</sup>Mechanical Engineering Department, University of Sistan and Baluchestan, P.O. Box 98164-161, Zahedan, Iran

Full list of author information is available at the end of the article

Brownian diffusion, sedimentation and dispersion may coexist in the main flow of a nanofluid. This means that the slip velocity between the fluid and particle may not be zero [22]. Therefore, it seems that the two-phase approach could better model nanofluid behaviours. Behzadmehr et al. [23] studied the turbulent forced convection of a nanofluid in a circular tube by using a two-phase approach. They implemented the two-phase mixture model for the first time to study nanofluid. Their comparison with the experimental results showed that the two-phase mixture model is more precise than the single-phase model. Mirmasoumi and Behzadmehr [24] studied the laminar mixed convection of a nanofluid in a horizontal tube using two-phase mixture model. They showed that the two-phase mixture model could better simulate the experimental results than the single-phase model. Recently, Lotfi et al. [25] studied two-phase Eulerian model that has been implemented to investigate such a flow field. Their comparison of calculated results with experimental values shows that the mixture model is more precise than the two-phase Eulerian model.

This work intends to investigate conjugate mixed convection-conduction of a nanofluid through an inclined tube. The tube is subjected to a uniform heat flux on its top surface; it is insulated on its bottom surface. Therefore, the effects of tube inclinations and particle volume fractions on the hydrodynamic and thermal parameters have been presented over a wide range of Re-Gr combinations.

### Mathematical formulation

Mixed convection of a nanofluid consists of water and  $Al_2O_3$  in a long copper tube with uniform heat flux at the top surface of tube wall has been considered. Figure 1 shows the geometry of the considered problem. The physical properties of the fluid are assumed constant except for the density in the body force, which varies linearly with the temperature (Boussinesq's hypothesis). Dissipation and pressure work are neglected. Thus, with these assumptions the conservation equations for steady state mixture model are as follows:

Continuity equation:

$$\nabla(\rho_{\text{eff}}V_m) = 0 \quad (1)$$

Momentum equation:

$$\nabla(\rho_{\text{eff}}V_mV_m) = -\nabla p + \nabla[\tau] + \nabla\left(\sum_{k=1}^n \phi_k \rho_k V_{\text{dr},k} V_{\text{dr},k}\right) - \rho_{\text{eff}} \beta_{\text{eff}} g(T - T_0) \quad (2)$$

Energy equation for fluid:

$$\nabla\left[\sum_{k=1}^n (\rho_k c_k) \phi_k V_k T\right] = \nabla(k_{\text{eff}} \nabla T) \quad (3)$$

The heat conduction throughout the solid wall:

$$k_s \nabla^2 T_s = 0 \quad (4)$$

Volume fraction:

$$\nabla(\phi_P \rho_P V_m) = -\nabla(\phi_P \rho_P V_{\text{dr},P}) \quad (5)$$

Where

$$V_m = \frac{\sum_{k=1}^n \phi_k \rho_k V_k}{\rho_{\text{eff}}}, \quad \tau = \mu_{\text{eff}} \nabla V_m \quad (6)$$

are the mean axial velocity and shear stress, respectively, and  $\phi$  is the volume fraction of phase k.

In Equation 2,  $V_{\text{dr},k}$  is the drift velocity for the secondary phase k, i.e. the nanoparticles in the present study:

$$V_{\text{dr},k} = V_k - V_m \quad (7)$$

The slip velocity (relative velocity) is defined as the velocity of a secondary phase (p) relative to the velocity of the primary phase (f):

$$V_{\text{pf}} = V_p - V_f \quad (8)$$

The drift velocity is related to the relative velocity:

$$V_{\text{dr},f} = V_{\text{pf}} - \sum_{k=1}^n \frac{\phi_k \rho_k}{\rho_{\text{eff}}} V_{\text{fk}} \quad (9)$$

The relative velocity is determined from Equation 10 proposed by Manninen et al. [26] while Equation 11 by Schiller and Naumann [27] is used to calculate the drag coefficient:

$$V_{\text{pf}} = \frac{\rho_p d_p^2}{18 \mu_f f_{\text{drag}}} \frac{(\rho_p - \rho_{\text{eff}})}{\rho_p} a \quad (10)$$

$$f_{\text{drag}} = \begin{cases} 1 + 0.015 Re_p^{0.687}, & Re_p \leq 1000 \\ 0.0183 Re_p, & Re_p > 1000 \end{cases} \quad (11)$$

The acceleration  $a$  in Equation 10 is:

$$a = g - (V_m \cdot \nabla) V_m \quad (12)$$

where:

$$Re_p = \frac{V_m d_p}{\nu_{\text{eff}}} \quad (13)$$

The physical properties in the above equations are: Effective density:

$$\rho_{\text{eff}} = (1 - \phi) \rho_f + \phi \rho_p \quad (14)$$

Chon et al. [12] correlation which considers the Brownian motion and nanoparticle mean diameter has been used for calculating the effective thermal conductivity:

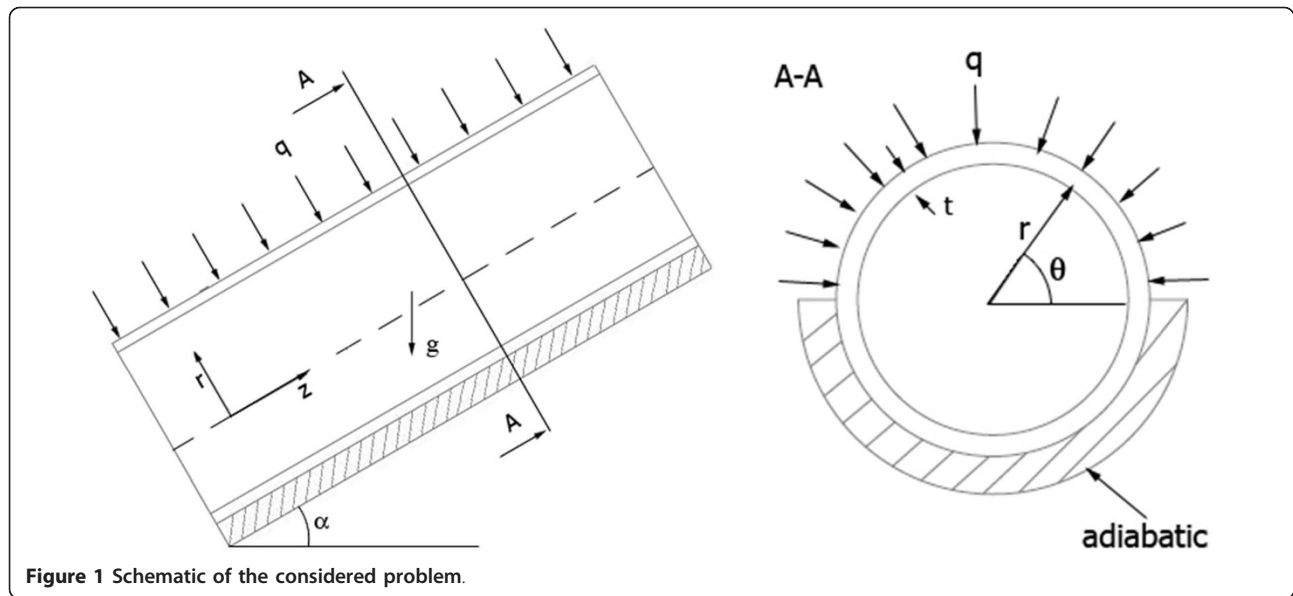


**Figure 1** Schematic of the considered problem.

$$\frac{k_{\text{eff}}}{k_f} = 1 + 64.7 \times \phi^{0.746} \left(\frac{d_f}{d_p}\right)^{0.369} \left(\frac{k_p}{k_f}\right)^{0.746} \times Pr^{0.9955} \times Re^{1.2321} \quad (15)$$

where  $Pr$  and  $Re$  in Equation 15 are defined as:

$$Pr = \frac{\mu_f}{\rho_f \alpha_f}, \quad Re = \frac{\rho_f B_c T}{3\pi \mu^2 L_f} \quad (16)$$

$L_f = 0.17$  nm is the mean free path of water,  $B_c$  is the Boltzmann constant ( $1.3807 \times 10^{-23}$  J/K) and  $\mu$  is calculated by the following equation:

$$\mu = A \times 10^{\frac{B}{T-C}}, \quad C = 140, \quad B = 247, \quad A = 2.414 \times 10^{-5} \quad (17)$$

Thermal expansion coefficient Khanafer et al. [16]:

$$\beta_{\text{eff}} = \left[ \frac{1}{1 + \frac{(1-\phi)\rho_f}{\phi\rho_p}} \frac{\beta_p}{\beta_f} + \frac{1}{1 + \frac{\phi\rho_p}{(1-\phi)\rho_f}} \right] \times \beta_f \quad (18)$$

An accurate equation is used for calculating the effective heat capacity [28].

$$(C_p)_{\text{eff}} = \left[ \frac{(1-\phi)(\rho C_p)_f + \phi(\rho C_p)_p}{\rho_{\text{eff}}} \right] \quad (19)$$

Effective viscosity is calculated by the following equation proposed by Masoumi et al. [15] which considers the effects of volume fraction, density and average diameters of nanoparticle and physical properties of the base fluid:

$$\mu_{\text{eff}} = \mu_f + \frac{\rho_p \times V_b d_p^2}{72C\delta}, \quad \delta = \sqrt{\frac{\pi}{6\phi}} d_p, \quad V_b = \frac{1}{d_p} \sqrt{\frac{18k_b T}{\pi \rho_p d_p}}, \quad C = \mu_f^{-1} [(c_1 d_p + c_2)\phi + (c_3 d_p + c_4)] \quad (20)$$

$c_1 = -0.000001133, c_2 = -0.000002771$   
 $c_3 = 0.00000009, c_4 = -0.000000393$

### Boundary condition

This set of nonlinear elliptical governing equations has been solved subject to the following boundary conditions:

At the tube inlet ( $Z = 0$ ):

$$V_{mz} = V_0, \quad V_{mr} = V_{m\theta} = 0, \quad T = T_0 \quad (21)$$

At ( $r = r_o$ )

$$0 \leq \theta \leq \pi : \quad -k_s \frac{\partial T_s}{\partial r} = q_w \quad (22)$$

$$\pi \leq \theta \leq 2\pi : \quad -k_s \frac{\partial T_s}{\partial r} = 0 \quad (23)$$

At the interface between the tube wall (copper) and the fluid ( $r = r_i$ ), the continuity condition for temperature and heat flux are applied so that:

$$T_w = T_{nf}, \quad k_s \frac{\partial T_w}{\partial r} = k_{\text{eff}} \frac{\partial T_{nf}}{\partial r}, \quad V_{mr} = V_{m\theta} = V_{mz} = 0 \quad (24)$$

At the tube outlet: atmospheric static pressure is assumed.

### Numerical method and validation

This set of coupled non-linear differential equations was discretized with the finite volume technique. For the convective and diffusive terms a second order upwind method was used while the SIMPLEC procedure was introduced for the velocity-pressure coupling. The discretization grid is uniform in the circumferential direction and non-uniform in the other two directions. It is finer near the tube entrance and near the wall where

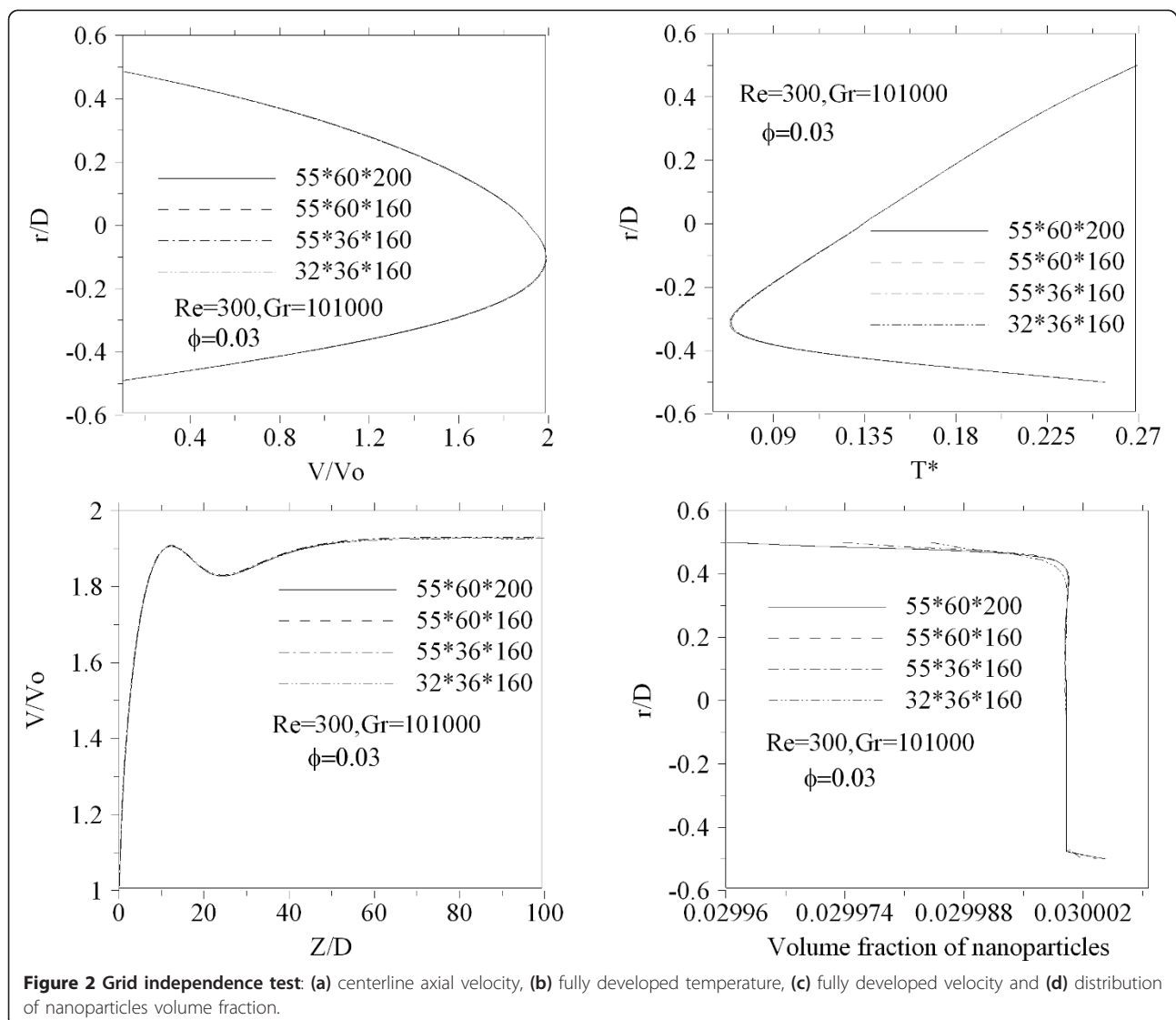
the velocity and temperature gradients are important. Several different grid distributions have been tested to ensure that the calculated results are grid independent. The selected grid for the present calculations consists of 160, 32 and 36 nodes, respectively, in the axial, radial and circumferential directions. As shown in Figure 2 increasing the grid numbers does not significantly change the velocity and temperature of the nanofluid. The grid test on the nanoparticle volume fraction is shown in Figure 2d. It is seen that the nanoparticle concentration does not change with increasing the grid numbers in the radial direction. Other axial and radial profiles have also been verified to be sure the results are grid independent.

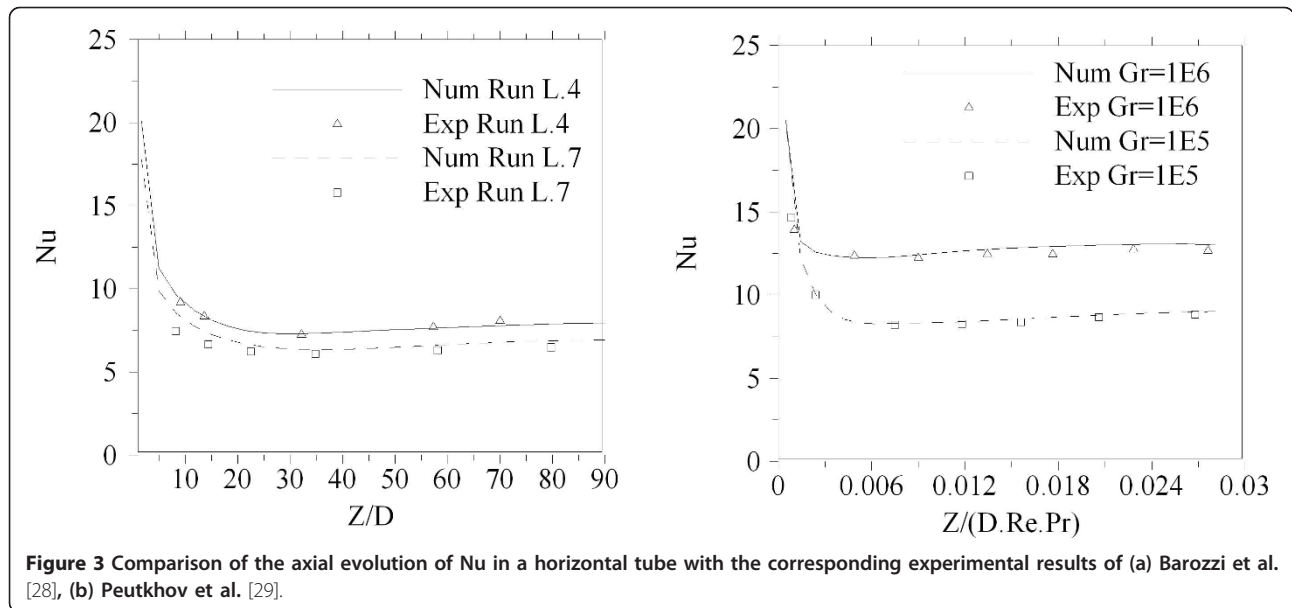
In order to demonstrate the validity and also precision of the model and the numerical procedure, comparisons

with the previously published experimental and numerical results have been done. Figure 3a,b shows the comparison of the calculated Nusselt number with the experimental results of Barozzi et al. [29] and Peutkhov et al. [30] in a horizontal tube, respectively. As shown good agreement between the results are seen.

A comparison has also been performed with the numerical results obtained by Ouzzane and Galanis [31]. As shown in Figure 4, axial evolution of the dimensionless temperatures and velocity is in good concordance with the present results.

It should be mentioned that our numerical results were obtained using the two-phase mixture model and considering a very small volume fraction for the solid particles. Therefore, the numerical procedure is reliable and can well predict developing mixed convection flow in a tube.



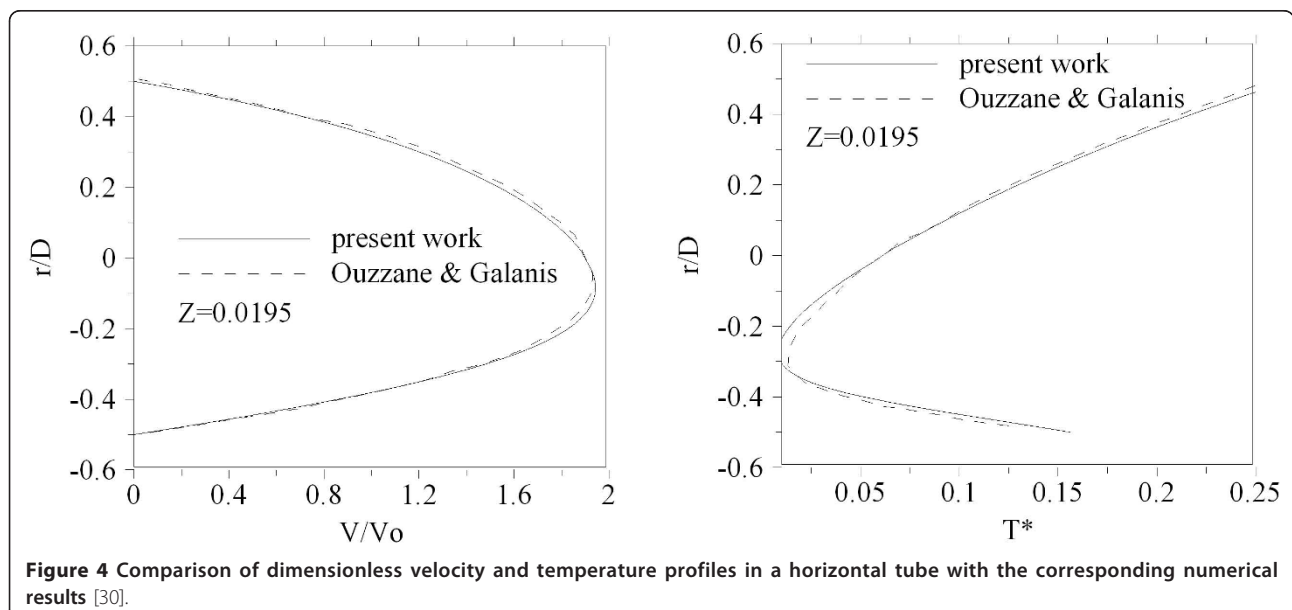


### Results and discussions

Calculations have been performed over wide range of  $Re-Gr$  combinations and nanoparticle concentrations. The Grashof number (or Richardson number) has been limited in order to respect the validity of the Boussinesq's approximation for the fluid density variation. The results presented here are for different Richardson numbers and three nanoparticle volume fractions.

For a given nanoparticle mean diameter and concentration ( $d_p = 28$  nm,  $\Phi = 0.04$ ) the effect of tube inclinations on the secondary flow vector and dimensionless temperature are shown in Figure 5 for two different Richardson numbers. As mentioned the tube is considered to be

made of copper which is a high thermal conductive metal. This transfers the heating energy from the top half surface of tube to the bottom half. Thus, the fluid at the bottom section could also be warm. The latter generates the secondary flow if it would be enough temperature differences. Since the warmer fluid tends to move upward and the colder goes down. In the case of higher Richardson number, the secondary flow is well established and significantly affects the fluid flow. Hot flow from the near wall region goes up and then backs downward at the centreline region. While at the lower  $Ri$ , where the circumferential temperature variation is low the strength of secondary flow is low. By tube inclination the warmer



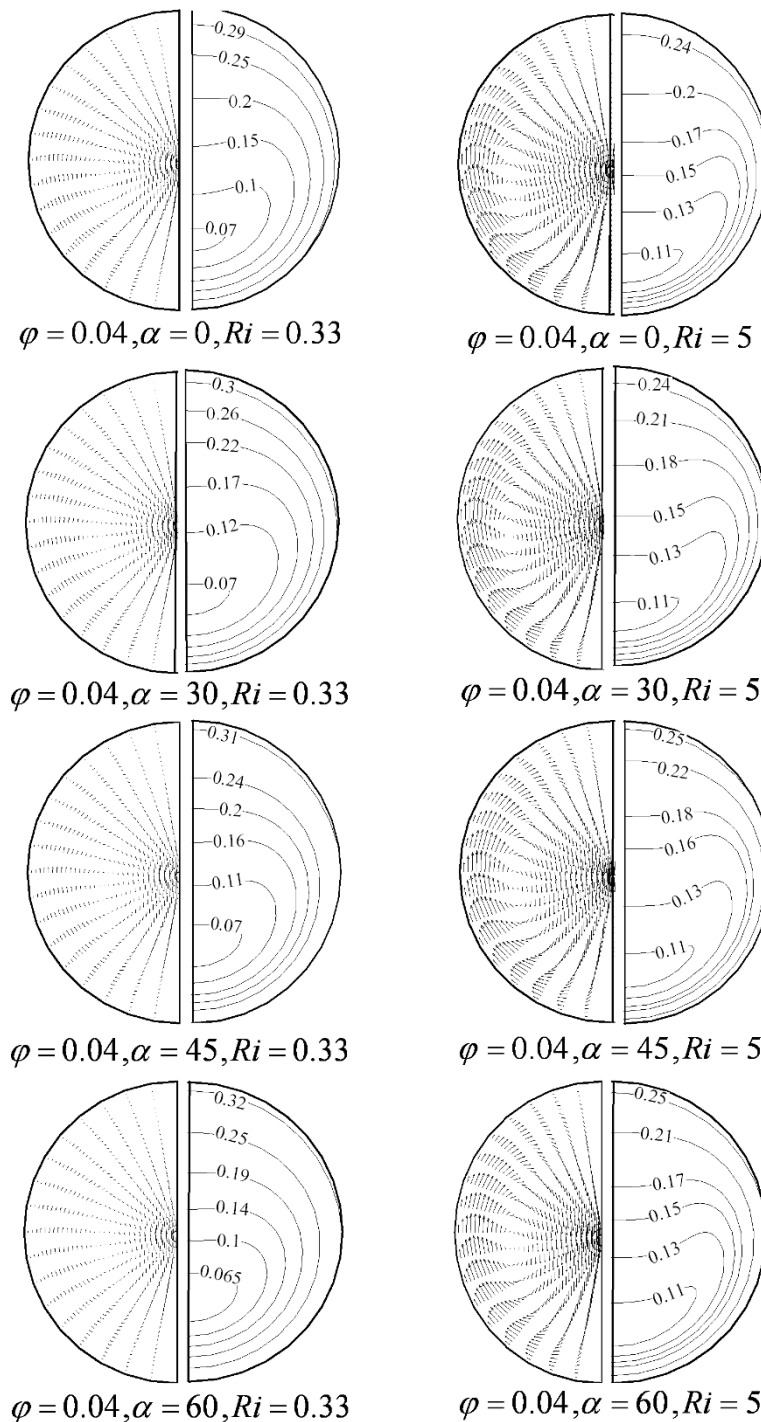


**Figure 5** Vectors of secondary flow and Contours of dimensionless temperature for different Ri and tube inclinations.

fluid is more accumulated at the upper part of tube because of decreasing secondary flow strength. Increasing the tube inclination augments the near wall axial buoyancy force while the radial component decreases. Thus, the strongest secondary flow vector is seen in the case of horizontal tube.

To see how the axial velocity profile is affected by the secondary flows, Figure 6 is presented. This figure shows the effect of tube inclination and the Richardson number on the axial velocity profile and dimensionless temperature profile. At  $\alpha = 0$ , increasing the Richardson number shifts the position of maximum axial velocity toward the

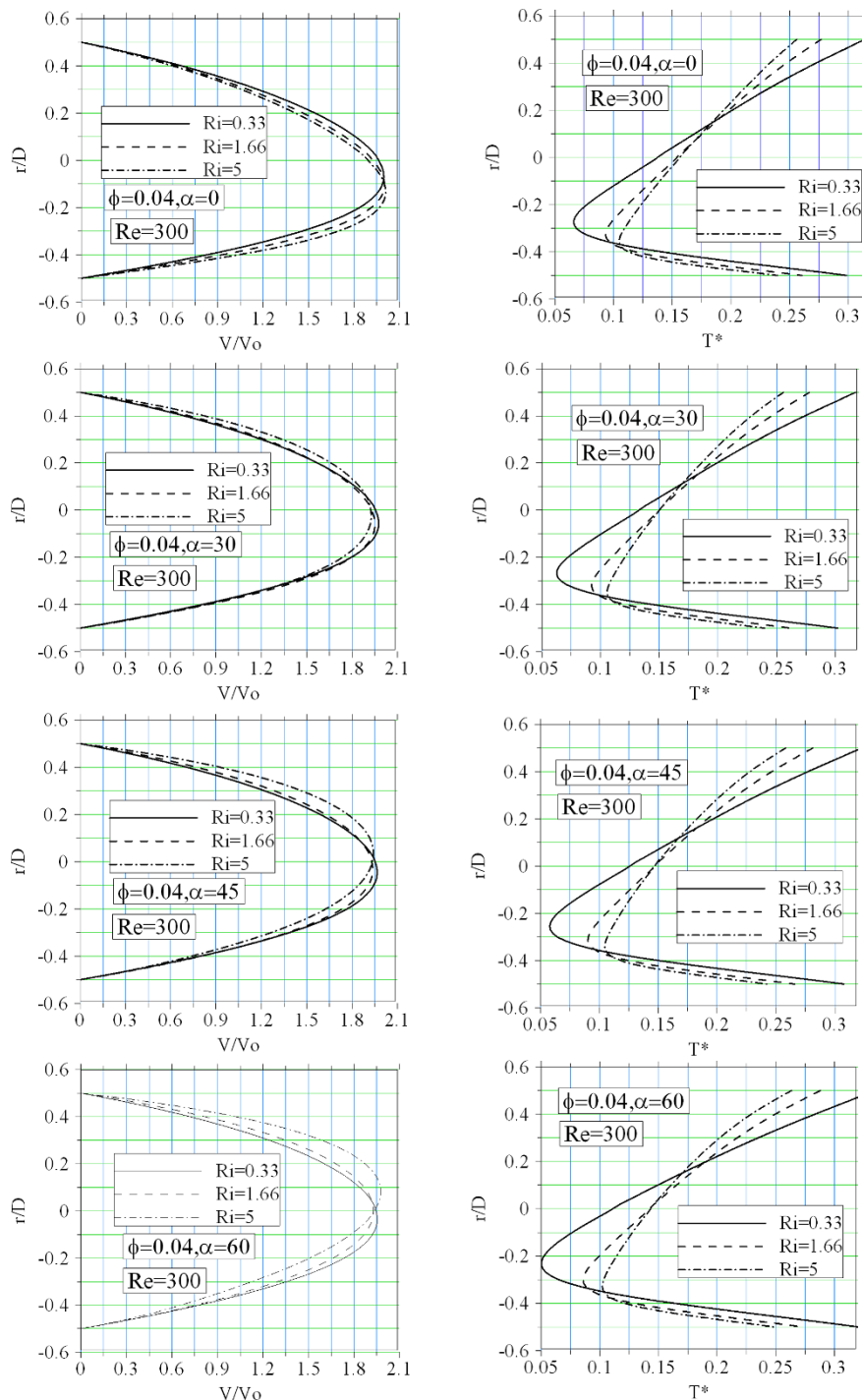


**Figure 6** Fully developed axial velocity and temperature profile.

bottom section. Since, the strength of secondary flow augments with the Richardson number. As intended, by increasing the Richardson number the bottom half of tube is also more affected by the energy that is transferred from the top half of tube. The temperature variation at the tube cross-section augments. By increasing the tube inclination

temperature variation at the tube cross-section becomes more uniform. The latter tends to shift the maximum axial velocity towards the upper part of tube. Where, axial component of the buoyancy forces is more important.

As seen in Figures 7 and 8, these forces and the secondary flow induced by the cross-sectional component of

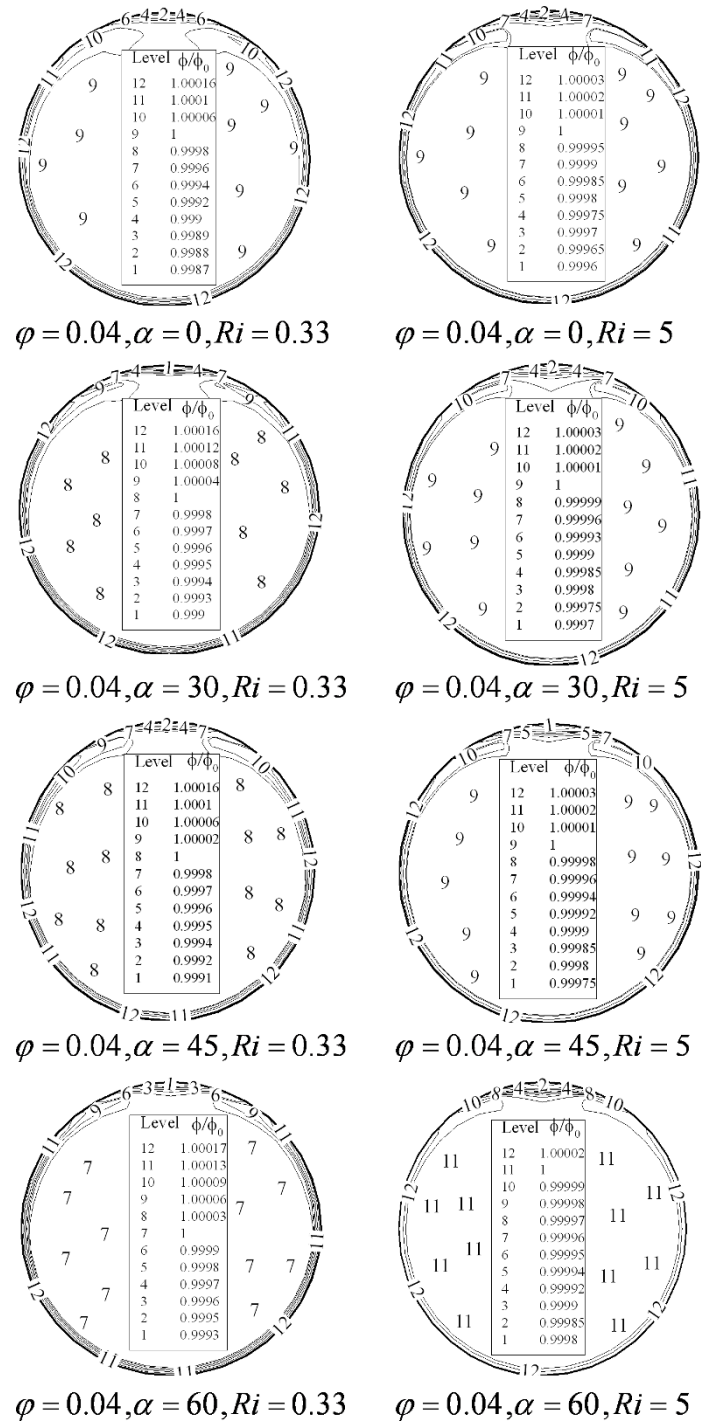


**Figure 7** Nanoparticles distribution at different Ri and tube inclinations.

the buoyancy forces affects the homogeneity of the dispersed nanoparticles. At the near wall region where the effect of viscous layer is more significant, nanoparticle concentration is more evident. In the other hand, secondary flow causes to see a region of lower nanoparticle concentration at the top of tube where the direction of

circular cell changes and goes back toward the bottom of tube. Thus, higher tube inclinations improve the homogeneity of the nanoparticles distribution. As shown in Figure 8 using larger particle accelerates the migration of the nanoparticle and deteriorates the nanofluid homogeneity. For the particles with smaller mean diameter, this



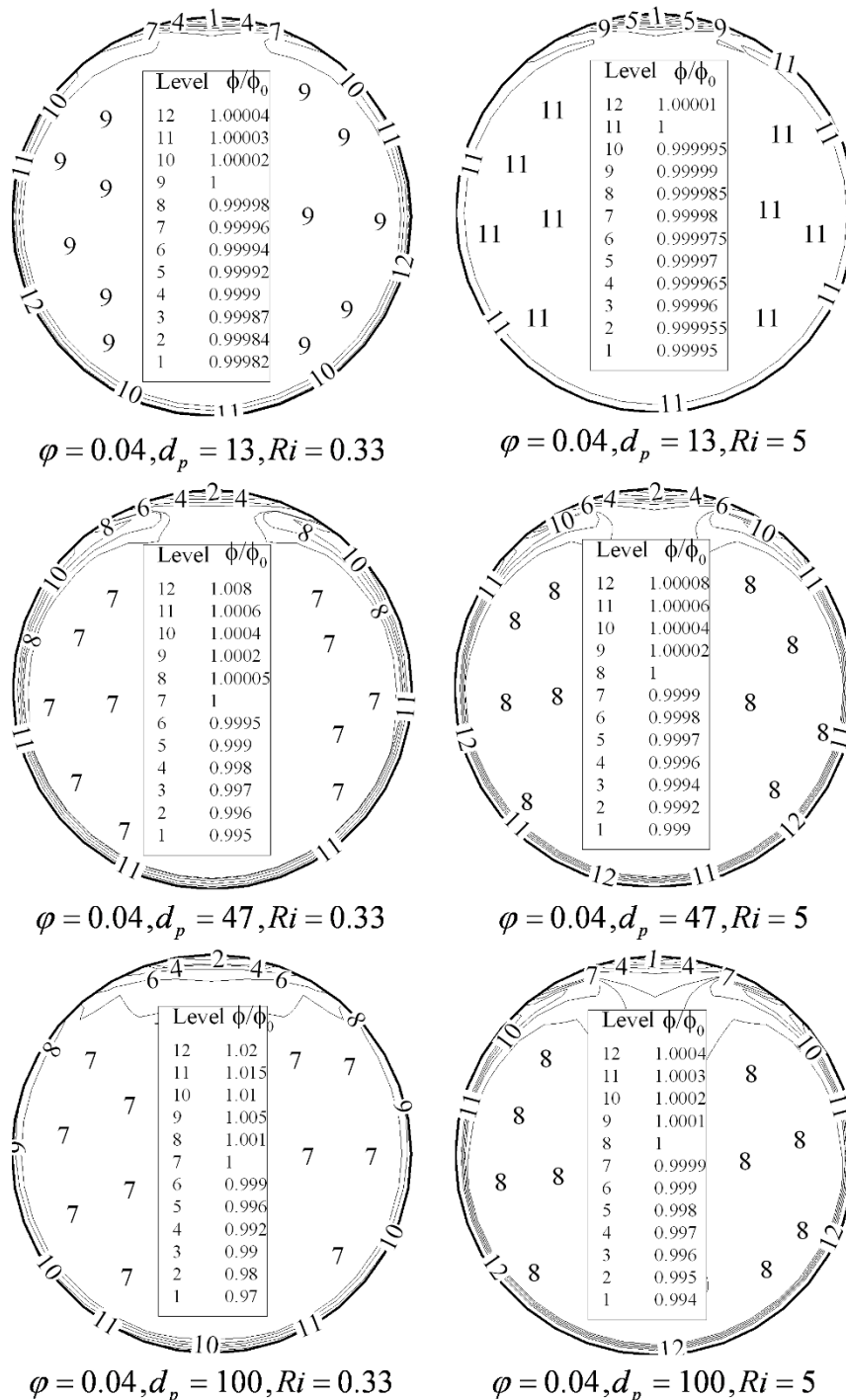


**Figure 8** Effect of nanoparticle mean diameter on the homogeneity of nanofluid.

variation is not significant and thus homogeneous distribution could be considered. While increasing nanoparticle mean diameter, non-uniformity on the particles distribution becomes more important and single-phase approach may fail. These effects could significantly affect heat transfer throughout the tube.

Axial evolution of the average peripheral convective heat transfer coefficient along the tube length is shown in Figure 9. In general  $h$  decreases and monotonically goes to its asymptotic value. Buoyancy forces components (axial and radial) significantly affected the variations of heat transfer coefficient. At the lower  $Ri$  for which the

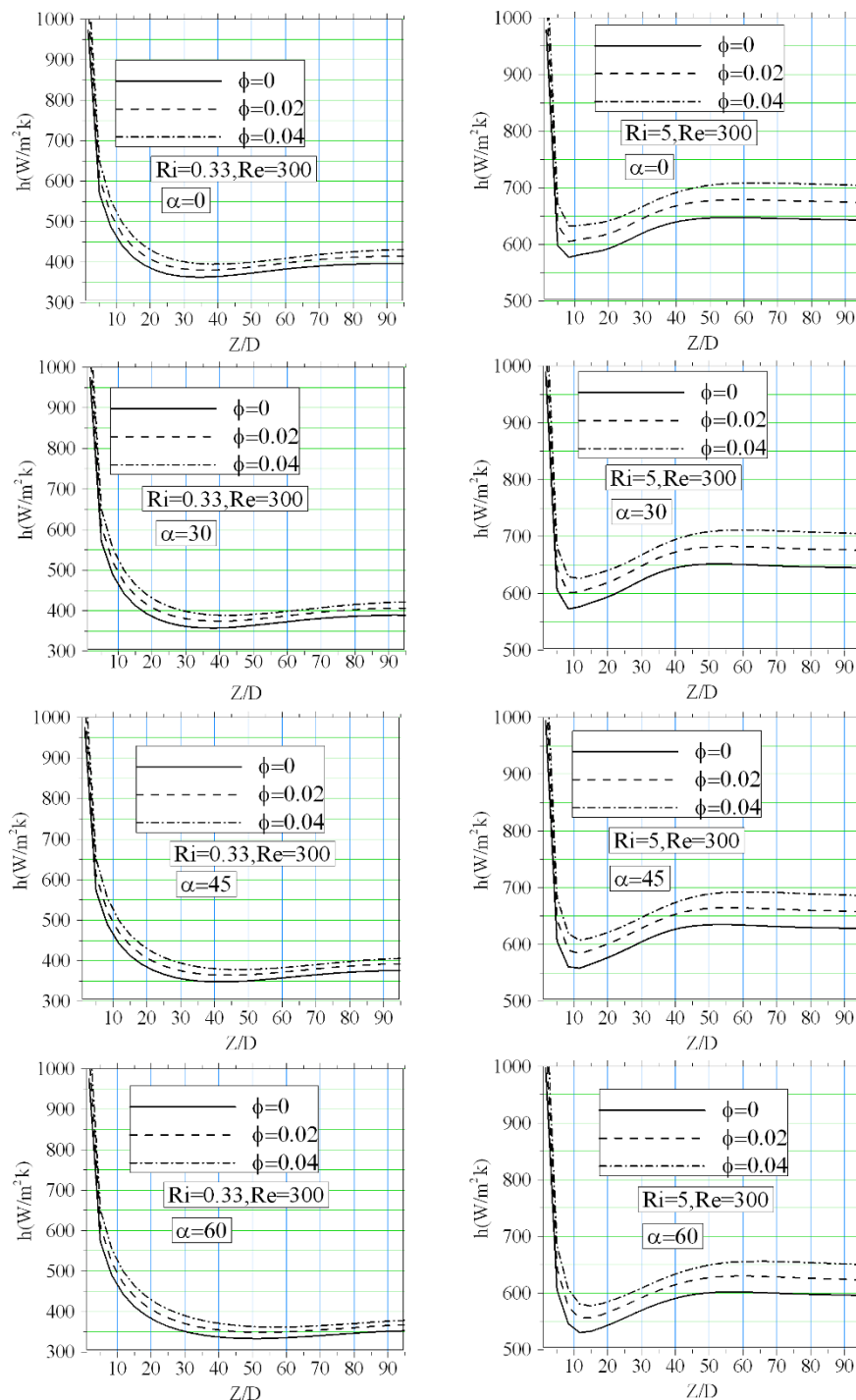


**Figure 9** Axial evolution of the peripheral average convective heat transfer coefficient.

effect of buoyancy force is weak, maximum heat transfer coefficient could be seen in the case of horizontal tube (pure radial buoyancy force). While at the higher Richardson number the buoyancy forces augments and so both axial and radial components become considerable. Based on the value of the axial and radial

components of the buoyancy force, the best tube inclination for which the highest heat transfer coefficient is achieved could be determined. For instance, at the low  $Ri$ , horizontal configuration gives the best heat transfer coefficient (among the other angle in Figure 9) while for the higher Richardson number ( $Ri = 5$ ) it appears at tube

inclination of  $\alpha = 30$ . This behaviour is also seen for different nanofluids. However, using nanofluid enhances heat transfer coefficient. This enhancement becomes more important at the higher Richardson number.

In spite of increasing heat transfer coefficient the peripheral average shear stress is also augmented. This is shown

in Figure 10 for different tube inclination and nanoparticle volume fraction. As seen, increasing nanoparticle concentration augments the shear stress which means more pumping power is needed for the fluid pumping. This partially arises from the fact that nanofluid viscosity increases with the nanoparticle concentration. The axial buoyancy

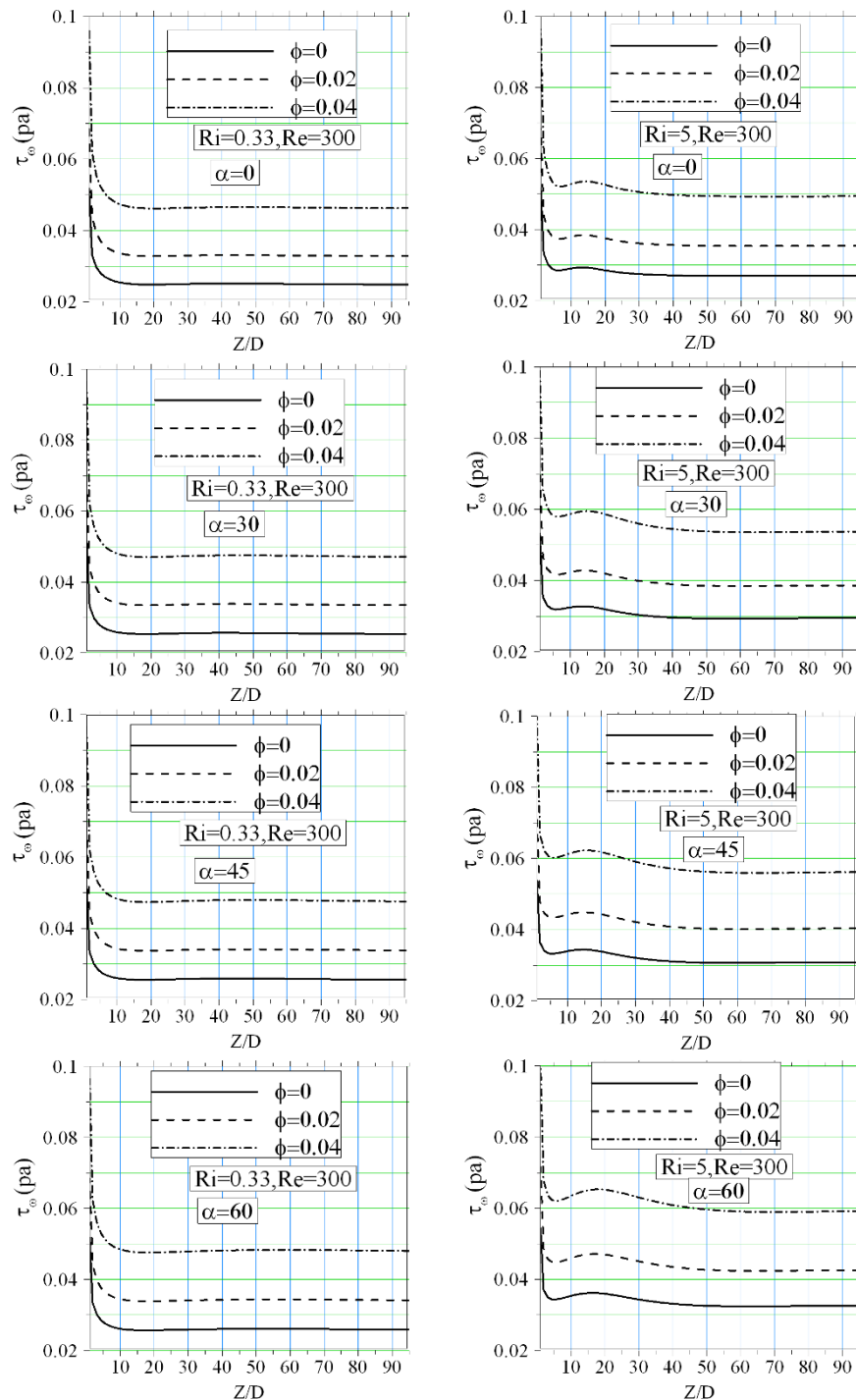


**Figure 10** Axial evolution of the peripheral average wall shear stress.

forces and near wall fluid acceleration has an important effect on the shear stresses. Thus, by increasing the tube inclinations axial buoyancy forces augments and the higher value of the average shear stress is observed. This is more evident in the case of higher Richardson number. To have a comparison between the heat transfer enhancement and pressure drop augmentation with nanoparticle concentration detail analysis of the corresponding data in the case of  $Re = 300$  and  $Ri = 5$ , is presented as an example. It shows that increasing the nanoparticle volume fraction from 0 to 2%, pressure drop augments by about 31% while the heat transfer coefficient increases by about 5%. This is showed that despite of stability and homogeneity of the nanofluids the pumping power is also an important concern that must be well addressed.

## Conclusion

Conjugate laminar mixed convection of water/ $Al_2O_3$  nanofluid in an inclined copper tube has been investigated numerically by using two-phase mixture model. The top half of tube wall is heated while the other half of tube is considered to be adiabatic. Copper is a good conductive material and transfers the heating energy from the upper part of tube to the lower half of tube by heat conduction mechanism. This could also increase the fluid temperature at this region. The latter could generate the secondary flow for which its strength depends on the nanoparticle volume fraction, the Richardson number and tube inclination angle. The buoyancy induced secondary flow augments with the nanoparticle volume fraction and the Richardson number. However, by tube inclination the axial component of the buoyancy forces increases and so the strength of secondary flow decreases. Nanoparticle concentration does not have significant effect on the axial velocity profile. However, at the high value of the Richardson number for which the effect of thermal energy is become more important than the hydrodynamic energy, nanoparticle concentration could affect the axial velocity profiles. Heat transfer coefficient is augmented with the nanoparticle volume fraction as well as the Richardson number. Combinations of the axial and radial component of the buoyancy forces could determine the inclination angle for which the maximum heat transfer enhancement occurs. However, the wall shear stress is significantly increased with the nanoparticle volume fraction. It is also augmented with the tube inclination because of increasing the axial component of the buoyancy forces.

## Abbreviations

**List of symbols:**  $C_p$ : Specific heat;  $D$ : Tube diameter (m);  $d_f$ : Molecular diameter of base fluid;  $d_p$ : Nanoparticle diameter (nm);  $E$ : Energy (J/kg);  $gd_f$ : Gravitational acceleration ( $ms^{-1}$ );  $Gr$ : Grashof number;  $h$ : convection heat transfer coefficient;  $k$ : Thermal conductivity (W/m K);  $P$ : Pressure (Pa);  $Pr$  Prandtl number;  $q''$ : Average heat flux at the solid-fluid interface ( $W/m^2$ );  $r$ :

Radial direction (m);  $r_i$ : Tube radial inner (m);  $r_o$ : Tube radial outer (m);  $Re$ : Reynolds number;  $Ri$ : Richardson number;  $T$ : Temperature (K);  $T^*$ : Temperature dimensionless;  $t$ : Thicknesses (m);  $V$ : Velocity (m/s);  $Z$ : Axial direction.

**Greek letters:**  $\alpha$ : Tube inclination;  $\beta$ : Volumetric expansion coefficient ( $K^{-1}$ );  $\theta$ : Angular coordinate;  $\phi$ : Volume fraction;  $\mu$ : Dynamic viscosity;  $\nu$ : Kinematic viscosity;  $\rho$ : Density;  $\tau$ : Shear stress.

**Subscripts:** b: Bulk; dr: Drift; eff: Effective; o: Outer condition; p: Particle; f: Base fluid; i: Inner condition; k: Summation index; m: Mixture; nf: Nanofluid; s: Solid; w: Interface; 0: Inlet condition.

## Author details

<sup>1</sup>Mechanical Engineering Department, University of Sistan and Baluchestan, P.O. Box 98164-161, Zahedan, Iran <sup>2</sup>Mechanical Engineering Department, Shahid Bahonar University, Kerman, Iran

## Authors' contributions

SA carried out the numerical simulation as a part of his master thesis which has been done under supervision of AB. SMS was adviser of the thesis. The authors have had regular scientific meeting and discussions during the work. All Authors read and approved the final manuscript.

## Competing interests

The authors declare that they have no competing interests.

Received: 29 October 2010 Accepted: 26 April 2011

Published: 26 April 2011

## References

1. Choi SUS: Enhancing thermal conductivity of fluid with nanoparticles. *ASME FED* 1995, **231**:99-105.
2. Xuan YM, Li Q: Heat transfer enhancement of nanofluids. *Int J Heat Fluid Flow* 2000, **21**:58-64.
3. Wen D, Ding Y: Experimental investigation into convective heat transfer of nanofluids at the entrance region under laminar flow conditions. *Int J Heat Mass Transfer* 2004, **47**:5181-5188.
4. Zeinali Heris S, Nasr Esfahany M, Etamad SGH: Experimental investigation of convective heat transfer of  $Al_2O_3$ /water nanofluid in circular tube. *Int J Heat Fluid Flow* 2006, **28**:203-210.
5. Fotukian SM, Nasr Esfahany M: Experimental investigation of turbulent convective heat transfer of dilute  $Al_2O_3$ /water nanofluid inside a circular tube. *Int J Heat Fluid Flow* 2010, **31**:606-661.
6. Prasher R, Bhattacharya P, Phelan PE: Brownian-motion-based convective-conductive model for the effective thermal conductivity of nanofluids. *ASME J Heat Transfer* 2006, **128**:588-595.
7. Shukla RK, Dhir VK: Study of the Effective Thermal Conductivity of Nanofluids. *Proceedings of the ASME IMECE, Orlando, FL, USA* 2005, 1-5.
8. Buongiorno J: A benchmark study on the thermal conductivity of nanofluids. *J Appl Phys* 2009, **106**:094312.
9. Lee S, Choi SUS, Li S, Eastman JA: Measuring thermal conductivity of fluids containing oxide nanoparticles. *J Heat Transfer* 1999, **121**:280-289.
10. Mints HA, Roy G, Nguyen CT, Doucet D: New temperature dependent thermal conductivity data for water based nanofluids. *Int J Therm Sci* 2009, **48**:363-371.
11. Sohrabi N, Masoumi N, Behzadmehr A, Sarvari SMH: A simple analytical model for calculating the effective thermal conductivity of nanofluids. *Heat Transfer Asian Res* 2010, **39**:141-150.
12. Chon CH, Kihm KD, Lee SP, Choi SUS: Empirical correlation finding the role of temperature and particle size for nanofluid ( $Al_2O_3$ ) thermal conductivity enhancement. *J Phys* 2005, **87**:1-3.
13. Murshed SMS, Leongand KC, Yang C: Investigations of Thermal Conductivity and Viscosity of Nanofluids. *Int J Therm Sci* 2008, **47**:560-568.
14. Nguyen CT, Desgranges F, Roy G, Galanis N, Maré T, Boucher S, Angue Mints HA: Viscosity data for  $Al_2O_3$ -water nanofluid-hysteresis: is heat transfer enhancement using nanofluids reliable? *Int J Therm Sci* 2008, **47**:103-111.
15. Masoumi N, Sohrabi N, Behzadmehr A: A new model for calculating the effective viscosity of nanofluids. *J Phys* 2009, **42**:055501.
16. Khanafer K, Vafai K, Lightstone M: Buoyancy-driven heat transfer enhancement in a two dimensional enclosure utilizing nanofluids. *Int J Heat Mass Transfer* 2003, **46**:3639-3653.

17. Akbari M, Behzadmehr A: Fully developed mixed convection in horizontal and inclined tubes with uniform heat flux using nanofluid. *Int J Heat Fluid Flow* 2007, **29**:566-586.
18. Bianco V, Manca O, Nardini S: Numerical investigation on nanofluids turbulent convection heat transfer inside a circular tube. *Int J Therm Sci* 2010, **1**-9.
19. Xuan YM, Roetzel W: Conceptions for heat transfer correlation of nanofluids. *Int J Heat Mass Transfer* 2000, **43**:3701-3707.
20. Mokmeli A, Saffar-Avval M: Prediction of nanofluid convective heat transfer using the dispersion model. *Int J Therm Sci* 2010, **49**:471-478.
21. Kumar S, Kumar Prasad S, Banerjee J: Analysis of flow and thermal field in nanofluid using a single phase thermal dispersion model. *Appl Math Model* 2010, **3**:573-592.
22. Xuan YM, Li Q: Investigation on convective heat transfer and flow features of nanofluids. *J Heat Transfer* 2003, **125**:151-155.
23. Behzadmehr A, Saffar-Avval M, Galanis N: Prediction of turbulent forced convection of a nanofluid in a tube with uniform heat flux using a two-phase approach. *Int J Heat Fluid Flow* 2007, **28**:211-219.
24. Mirmasoumi A, Behzadmehr A: Numerical study of laminar mixed convection of a nanofluid in a horizontal tube using two-phase mixture model. *Appl Therm Eng* 2008, **77**:717-727.
25. Lotfi R, Saboohi Y, Rashidi AM: Numerical study of forced convective heat transfer of Nanofluids: Comparison of different approaches. *Int Commun Heat Mass Transfer* 2010, **37**:74-78.
26. Manninen M, Taivassalo V, Kallio S: On the Mixture Model for Multiphase Flow. *Technical Research Center of Finland, VTT Publications* 1996, **288**:9-18.
27. Schiller L, Naumann A: A drag coefficient correlation. *Z Ver Deutsch Ing* 1935, **77**:318-320.
28. Zhou SQ, Ni R: Measurement of the specific heat capacity of water-based Al<sub>2</sub>O<sub>3</sub> nanofluid. *Appl Phys Lett* 2008, **92**:093123.
29. Barozzi GS, Zanchini E, Mariotti M: Experimental investigation of combined forced and free convection in horizontal and inclined tubes. *Int J Mech* 1985, **20**:18-27.
30. Petukhov BS, Polyakov AF: Experimental Investigation of Viscogravitational Fluid Flow in a Horizontal Tube. Scientific Research Institute of High Temperatures, translated from *Teplofizika Vysokikh Temperature*. 1967, **5**:87-95.
31. Ouzzane M, Galanis N: Developing mixed convection in an Inclined tube with circumferentially nonuniform heating at its outer surface. *J Numer Heat Transfer* 1999, **35**:609-628.

doi:10.1186/1556-276X-6-360

Cite this article as: Allahyari et al.: Conjugate heat transfer of laminar mixed convection of a nanofluid through an inclined tube with circumferentially non-uniform heating. *Nanoscale Research Letters* 2011 **6**:360.

Submit your manuscript to a SpringerOpen® journal and benefit from:

- Convenient online submission
- Rigorous peer review
- Immediate publication on acceptance
- Open access: articles freely available online
- High visibility within the field
- Retaining the copyright to your article

---

Submit your next manuscript at ► [springeropen.com](http://springeropen.com)

---